APPLIED ORGANOMETALLIC CHEMISTRY
Appl. Organometal. Chem. 2004; **18**: 337–342
Published online in Wiley InterScience (www.interscience.wiley.com). DOI:10.1002/aoc.636

Laser-induced synthesis of iron–iron oxide/methylmethoxysilicone nanocomposite

Josef Pola[1]*, Zdeněk Bastl[2], Vladimír Vorlíček[3], Florian Dumitrache[4], Rodica Alexandrescu[4], Ion Morjan[4], Ion Sandu[4] and Victor Ciupina[5]

[1]Laser Chemistry Group, Institute of Chemical Process Fundamentals, Academy of Sciences of the Czech Republic, 165 02 Prague 6, Czech Republic
[2]J. Heyrovsky Institute of Physical Chemistry, Academy of Sciences of the Czech Republic, 182 23 Prague 8, Czech Republic,
[3]Institute of Physics, Academy of Sciences of the Czech Republic, 180 40 Prague, Czech Republic
[4]National Institute for Lasers, Plasma and Radiation Physics, PO Box MG-36, R-76900 Bucharest, Romania
[5]Ovidius University of Constanta, POB 8600, Constanta, Romania

Received 14 October 2003; Accepted 29 January 2004

The IR laser irradiation of a gaseous mixture of iron pentacarbonyl–methoxytrimethylsilane–ethene in argon induces ethene-photosensitized decomposition of iron pentacarbonyl into elemental iron and decomposition of methyltrimethoxysilane into species that polymerize into methylmethoxysilicone. These two concurrent gas-phase processes allow formation of iron–iron oxide/methylmethoxysilicone nanocomposite. Spectral analyses and electron microscopy reveal the nanocomposite as consisting of iron clusters oxidized in outer layers and covered with the organosilicon polymer. The procedure shows its potential for gas-phase synthesis of iron-based clusters embedded in a polymer matrix.

KEYWORDS: laser-induced decomposition; iron pentacarbonyl; methoxytrimethylsilane; gas-phase chemistry; iron–iron oxide/methylmethoxysilicone nanocomposite; gas-phase polymerization

INTRODUCTION

There is continuing interest in hybrid organic–inorganic materials[1] and incorporation of small metal and metal-based particles into inorganic and polymeric matrices.[2] This is motivated by the unique properties and promising applications of these materials. One of the interesting classes of these materials is magnetic nanocomposites, which are comprised of a magnetic and a nonmagnetic species and in which the magnetic properties can be tailored by means of composition and processing variables.[3] These nanocomposites were produced by incorporating different metals or metal oxides in inorganic (e.g. silicon oxide,[4] porous glass,[5] mesopouros silica[6]) and organic (different polymeric[7–12]) matrices.

*Correspondence to: Josef Pola, Laser Chemistry Group, Institute of Chemical Process Fundamentals, Academy of Sciences of the Czech Republic, 165 02 Prague 6, Czech Republic.
E-mail: pola@icpf.cas.cz
Contract/grant sponsor: Grant Agency of Academy of Sciences; Contract/grant number: A4072107.
Contract/grant sponsor: Ministry of Education, Youth and Sports; Contract/grant number: OC 523.60.

The incorporation of magnetic iron oxide (Fe_2O_3) nanoclusters into organic polymers has been achieved through static casting,[13] by a wet chemical approach,[14] using ultrasound radiation,[15] by *in situ* oxidation of iron salts within polymer latex,[16] by seed precipitation polymerization in the presence of iron oxide nanoparticles[17,18] and also by laser-vaporization of metals into ultrafine metal and cationic particles that act as polymerization catalysts.[19] Also, zero-valent iron nanoparticles stabilized by polymers have been prepared by sonolysis of a solution of iron pentacarbonyl ($Fe(CO)_5$) in anisol in the presence of poly(dimethylphenyleneoxide).[20]

IR laser-induced and sulfur hexafluoride (SF_6)- or ethene (C_2H_4)-photosensitized gas-phase decomposition of $Fe(CO)_5$ is well known for its potential to serve for chemical vapour deposition of nanostructured iron[21–25] or, when carried out in the presence of air or N_2O, for chemical vapour deposition of iron oxide (Fe_2O_3)[23–28] particles.

This technique has not yet been applied successfully to chemical vapour deposition of iron (or Fe_2O_3)–polymer nanocomposites, although concurrent UV laser-induced gas-phase decomposition of an organometallic compound to metal clusters and polymerization of a monomer has been documented.[29] Thus, IR laser irradiation of gaseous mixtures

of silane and $Fe(CO)_5$ does not result in dehydrogenative coupling of transient silylene (leading to polysilene), but instead yields silicon–iron powders;[30,31] similarly, IR laser irradiation of gaseous $Fe(CO)_5$–SF_6–silacyclopent-3-ene (polymer precursor) yields Fe(CO)-containing unsaturated polymer.[32]

Successful IR laser gas-phase synthesis of iron or (Fe_2O_3)–polymer nanocomposites must involve (i) a complete removal of CO ligands from $Fe(CO)_5$ and (ii) a concurrent polymerization of suitable volatile organic monomer. The reaction temperature in the IR laser pyrolysis often exceeds 700–800 °C. This temperature is considerably higher than that required for the decomposition of $Fe(CO)_5$ (around 350 °C[33]), but is very feasible for degradation (carbonization) of common polymers. The technique may thus seem of limited value for synthesis of iron–polymer composites.

Some of our previous studies on UV and IR laser-induced chemical vapour deposition of alkylsilicone polymers[34–37] have shown these polymers to be thermally superior materials and to be able to withstand temperatures up to 800 °C.[38–41] Our previous findings thus allow us now to report that IR laser irradiation of a gaseous pentacarbonyl–C_2H_4–(methoxy)trimethylsilane ($(CH_3)_3SiOCH_3$) mixture leads to synthesis of ultrafine iron–iron oxide/organosilicon polymer nanocomposite that is obtained due to simultaneous formation of iron clusters from $Fe(CO)_5$ and of organosilicon polymer from $(CH_3)_3SiOCH_3$. The characterization of the powders by a number of techniques is in line with superficial oxidation of iron clusters that are embedded into the organosilicon polymer.

EXPERIMENTAL

The experimental set-up (Fig. 1) consisted of a flow reactor equipped with NaCl windows and a continuous-wave (c.w.) CO_2 laser. The vapours of $Fe(CO)_5$ and $(CH_3)_3SiOCH_3$ (each diluted with C_2H_4) together with argon (needed for gas and particle confinement) were separately introduced into the reaction chamber through three concentric nozzles at a total pressure 520 mbar. The flow rates of $Fe(CO)_5$–C_2H_4, $(CH_3)_3SiOCH_3$–C_2H_4, argon admitted to the reactor centre and argon introduced to the windows were 85 sccm, 30 sccm, 1100 sccm and 250 sccm respectively. The laser beam (output power 90 W, $\lambda = 10.6$ μm) was mildly focused by an NaCl lens to achieve an energy density of 2.2 kW cm^{-2} when crossed with the reactant flow. These conditions gave 0.38 g of an ultrafine black powder on a filter after 30 min irradiation.

The black ultrafine powder obtained was transferred for measurements of its properties by FTIR, Raman and electron paramagnetic resonance (EPR) and X-ray photoelectron spectroscopics and electron microscopy.

The FTIR spectra were obtained on powder in KBr pellets using a Nicolet Impact 400 spectrometer.

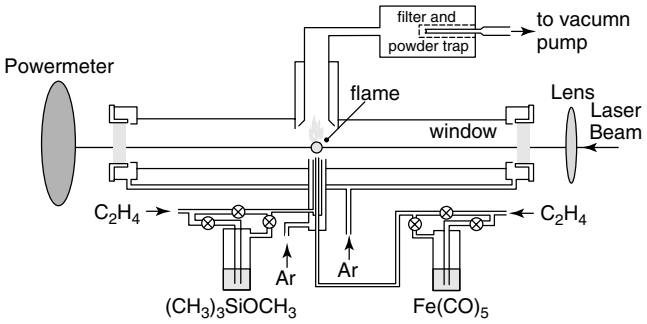

Figure 1. Scheme of experimental set-up.

The Raman spectra were recorded on a Renishaw (a Ramascope model 1000) Raman microscope coupled with a CCD detector. The excitation beam of an argon-ion laser was defocused to obtain an energy density lower than 4×10^3 W cm^{-2} and to diminish the heating of the sample.

The EPR spectra were registered on a c.w. X-band spectrometer at room temperature at a microwave power level of 1 mW and with 100 kHz modulation of 0.115 mT.

Scanning electron photomicrographs were obtained using a Philips XL30 CP scanning electron microscope and transmission electron photomicrographs on samples were recorded by using a Philips 201 and CM 120 transmission electron microscopes.

X-ray photoelectron spectra were measured with a Gammadata Scienta ESCA 310 electron spectrometer using monochromatized Al Kα ($h\nu = 1486.6$ eV) radiation for electron excitation. The energy scale of the spectrometer was calibrated with Au $4f_{7/2}$ binding energy fixed at 84.0 eV. The high-resolution spectra of Fe 2p, Si 2p, C 1s and O 1s photoelectrons were measured for an as-received sample and after mild Ar^+ ion sputtering ($E = 6$ keV, $I = 10$ μA, $t = 3$ min). The ratios of atomic elemental concentrations were calculated assuming a homogeneous sample.

Thermogravimetric analysis of the solid deposit (sample weight 33 mg) was carried out by heating the sample to 700 °C at a rate of 4 °C min^{-1}, using Cahn D-200 recording microbalances in a stream of argon. The sample residue was analysed in a KBr pellet by FTIR spectroscopy.

$Fe(CO)_5$, C_2H_4 and argon (purity 99.9%) were purchased from Aldrich and $(CH_3)_3SiOCH_3$ (better than 95% purity) was from laboratory stock.

RESULTS AND DISCUSSION

The c.w. CO_2 laser irradiation of the $Fe(CO)_5$–C_2H_4–$(CH_3)_3SiOCH_3$–Ar mixture was accompanied by the occurrence of a clear white flame observed above the nozzle introducing the gaseous mixture and by the occurrence of the gas-phase formation of a black powder that was carried out vertically and trapped and accumulated on the filter. This laser synthesis technique, known as laser pyrolysis,[42–44]

is based on the excitation of C_2H_4 and collisional energy transfer between the excited C_2H_4 molecules and non-absorbing molecules of $Fe(CO)_5$ and $(CH_3)_3SiOCH_3$, which both being enriched in energy undergo decomposition. These decompositions occur in a small, well-confined irradiation volume, defined by the intersection of the laser beam with the inlet gas flow, and have different courses. The IR laser decomposition of $Fe(CO)_5$ results[21–25] in the formation of elemental iron and CO, whereas the decomposition of $(CH_3)_3SiOCH_3$ proceeds[45] via initial cleavage of the Si–C and O–C bonds to produce dimethylsilanone transients which then yield[46] into methylsilicone polymer. These steps, as well as cleavage of the C–H bonds and the recombination of the thus-produced carbon- and silicon-centred radicals, are plausible reactions.[38–41] These reactions (Scheme 1) are known[38–41,45] to yield organosilicon polymers incorporating both $-Si(CH_3)_2-O-Si(CH_3)_2-$ and $-Si(CH_3)_2-CH_2-Si(CH_3)_2-$ linkages (respectively referred in Scheme 1 to as methoxymethylsiloxane and methoxymethylcarbosilane structures).

The laser heating of the $Fe(CO)_5-C_2H_4-(CH_3)_3SiOCH_3-Ar$ mixture thus induces formation of elemental iron and methylmethoxysiloxane/carbosilane polymer, both of which combine to form a composite. These inferences are in line with analyses of the solid material presented below.

The FTIR spectrum of the black powder (Fig. 2a) consists of absorption bands typical[47] for methyl(methoxy)siloxane structures (at 1037, 1064, 1115, 1166 and 2918 cm^{-1}) containing $Si-OCH_3$ groups (ν_{C-H} at 2849 cm^{-1} and ν_{C-O-Si} at above 1100 cm^{-1}) and possibly $Si-CH_2-Si$ moieties (1035 cm^{-1}).[48] The latter moieties would indicate that $(CH_3)_3SiOCH_3$ also decomposes via C–H bond splits and recombination of silicon and carbon-centred radicals (Scheme 1). The spectra do not show any absorption bands of iron oxide (Fe_2O_3 bands at 550–700 cm^{-1}),[49] which could be due to a low occurrence of Fe_2O_3 and/or the low relative absorptivity of these bands.

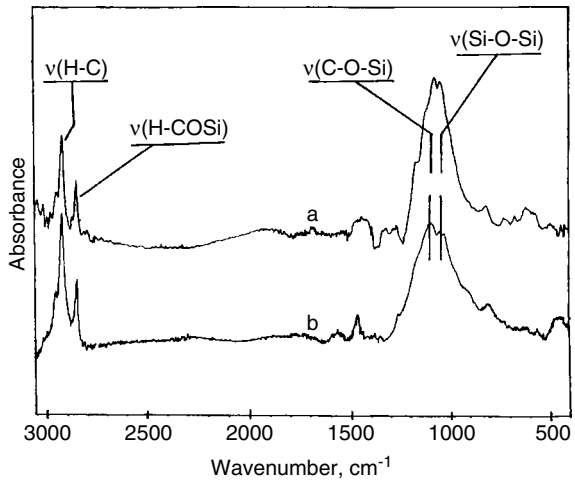

Figure 2. FTIR spectrum of black powder before (a) and after (b) heating to 800 °C.

The Raman spectra of the black powder obtained for different micro-regions (Fig. 3) show different patterns, revealing that the material is not completely homogeneous. They display bands characteristic[50–52] of α-Fe_2O_3 (bands 1–3, 4 and 7 at 217–221 cm^{-1}, 281–287 cm^{-1}, 391–405 cm^{-1}, 483–494 cm^{-1} and 1315 cm^{-1} respectively) and of γ-Fe_2O_3 and/or Fe_3O_4 (bands 3, 5 and 6 at 391–405 cm^{-1}, 600 cm^{-1} and 670 cm^{-1} respectively). In addition, the spectra reveal a band corresponding to disordered carbon (band 8). We judge that the carbon originates from a very minor decomposition of C_2H_4.

X-ray photoelectron spectra taken before and after ion sputtering are consistent with the stoichiometry of superficial

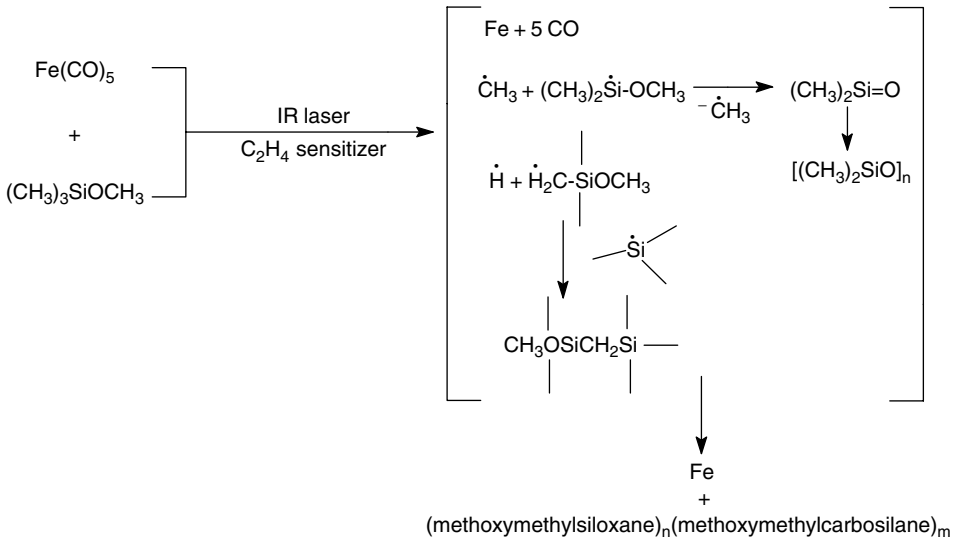

Scheme 1. Decomposition steps in the irradiated mixture.

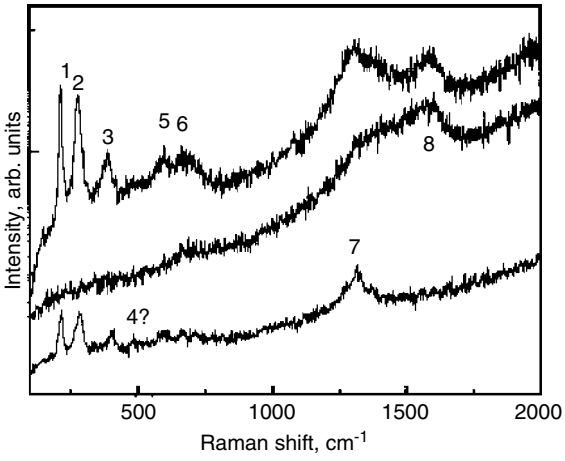

Figure 3. Raman spectra of black powder for different micro-regions.

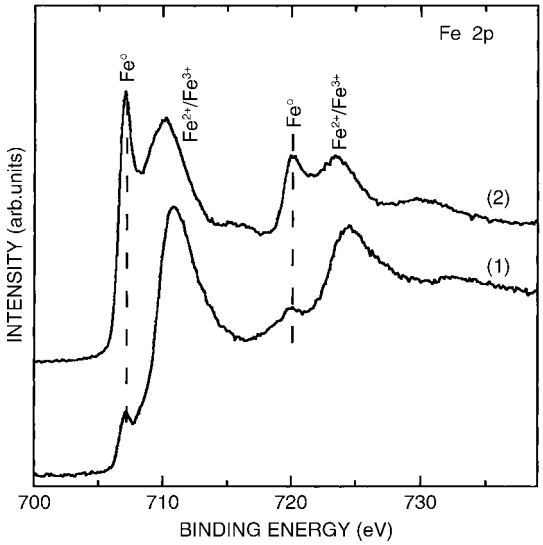

Figure 4. X-ray photoelectron spectrum of black powder before (1) and after (2) argon-ion sputtering.

layers equal to $Si_{1.0}O_{3.66}C_{1.95}Fe_{0.68}$ and $Si_{1.0}O_{3.65}C_{1.23}Fe_{3.20}$ respectively. They reveal that most of the iron is present in two chemical states (Fig. 4), i.e. elemental iron (Fe $2p_{3/2}$ binding energy 707.0 ± 0.2 eV)[53] and Fe_2O_3 (Fe $2p_{3/2}$ binding energy 711.2 ± 0.2 eV).[54] The mild ion sputtering results in a significant increase of total iron concentration and in an increase of the elemental iron from 6 to 16%. Simultaneously, the signal of the iron oxide constituent is shifted to lower values (709.9 ± 0.2 eV) and contains a satellite structure characteristic[55] of Fe^{2+}. The spectra of C 1s electrons of the sputtered sample show that about 40% of carbon is present in the carbidic state. The iron carbide is likely produced in chemical reaction induced by argon ion irradiation. The Si 2p core-level binding energy, 102.2 ± 0.2 eV, is consistent[56] with silicon contained in polysiloxane $[-Si(C_xH_y)_2-O-]_n$ structures. The X-ray photoelectron spectra measured are thus fully consistent with an iron component having an Fe^0 core, which becomes progressively oxidized as one moving from the inner to the outermost layers, and which is covered with an organosilicon polymer layer <10 nm thick.

Scanning electron microscopy analysis reveals that the powder consists of compact agglomerates that are formed by fluffy structures (Fig. 5). The electron diffraction pattern (Fig. 6a) reveals interlayer distances at 2.59. 2.09, 1.75, 1.54 and 1.50 Å, which is in keeping with crystalline maghemite, and haematite Fe_2O_3 and α-Fe phase. Transmission electron spectroscopy images (Fig. 6b–d) are compatible with cross-linked chains of *ca* 20 nm in diameter that are formed by iron/iron oxide particles, several nanometers in size, coated with organosilicon polymer (Fig. 6c).

The significant oxidation of iron nanoparticles proven by Raman and photoelectron spectra can be explained in terms of incomplete coverage of the iron cores by the polymer, or by complete coverage with a porous polymeric shell. In both cases the iron particles will be easily oxidized when exposed to atmosphere.

Thermogravimetric analysis of the powder revealed its high thermal stability. Thus, the powder heated to 700 °C liberates methane and ethyne (1.7% and 0.1% of total weight respectively) and its weight remains virtually unchanged. This thermal behaviour is compatible[38–41] with the superior thermal stability of alkysilicones laser-prepared from disiloxanes and alkoxysilanes. A small modification of the FTIR spectral pattern upon this heating (Fig. 2b) is in line with minor structural changes within the polymer skeleton.

We remark that the material obtained is interesting because of its magnetic properties, since it represents a magnetic nanocomposite comprised of magnetic and nonmagnetic species whose properties can be tailored by means of composition and processing variables.[57] The nanocomposite material obtained can also find important use in sensor applications. Iron oxides have recently been found to be promising candidates for a new generation of gas sensors with high sensitivity and specific selectivity,[58–60] and their properties can be considerably enhanced in nanostructured systems, leading to increased specific surface.

More work is under way to explore the possibility of synthesis of iron particles that are completely covered and stabilized within the polymer core.

CONCLUSIONS

Nanocomposite iron–iron oxide/organosilicon polymers were prepared for the first time by IR laser-induced and C_2H_4-photosensitized co-decomposition of $Fe(CO)_5$ and $(CH_3)_3SiOCH_3$. The procedure allows concurrent gas-phase formation of iron nanoparticles and of efficiently polymerizing organosilicon transients. It shows great potential for the

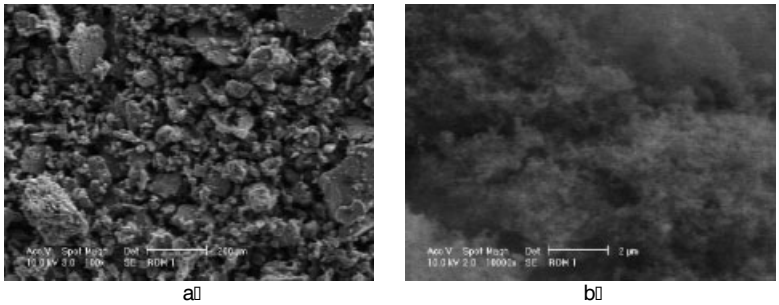

Figure 5. SEM images of powder; bar: 200 μm (a) and 2 μm (b).

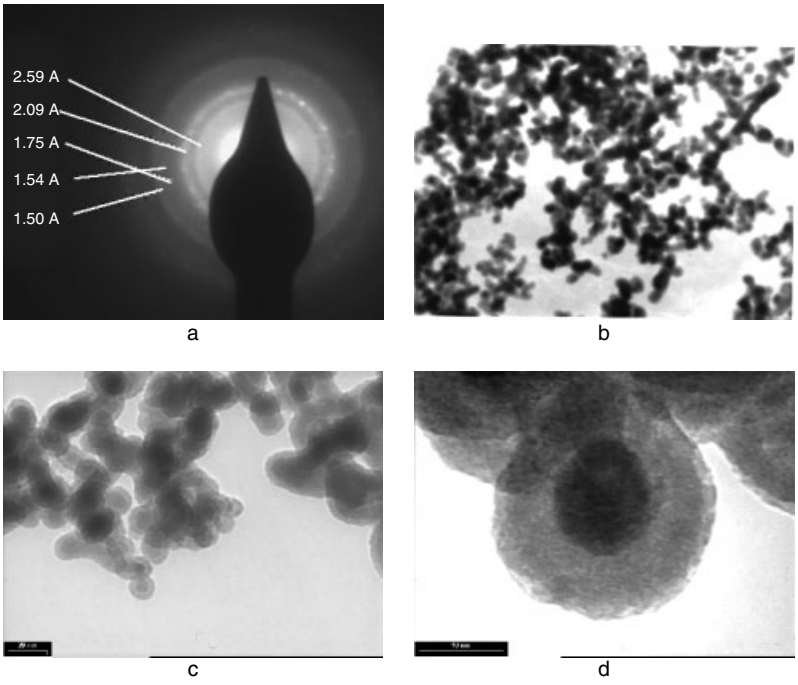

Figure 6. Electron diffraction image (a) and transmission electron microscope images (b)–(d) of the powder. Magnification: (b) 100 000×; (c) bar = 20 nm; (d) bar = 10 nm.

gas-phase synthesis of iron-based clusters embedded in an organosilicon polymer matrix.

The nanocomposite undergoes oxidation when exposed to air and it can be described as an organosilicon polymer with embedded iron nanoparticles having a zero-valent iron core and increasing content of iron oxides when going from the inner to outermost layers. The material obtained is interesting in view of its potential to act as a very sensitive gas sensor.

Acknowledgements

The work was supported by GAAVCR (grant A4072107) and by the Ministry of Education, Youth and Sports (grant no. OC 523.60) of the Czech Republic. We thank Dr Anna Galikova and Dr Aftanas Galik for the thermogravimetric analysis.

REFERENCES

1. Corriu R. *Angew. Chem. Int. Ed. Engl.* 1996; **35**: 1420.
2. Sergeev GB, Petrukhina MA. *Progr. Solid State Chem.* 1996; **24**: 183.
3. Shull RD, Bennett LH. *Nanostruct. Mater.* 1992; **1**: 83.
4. Shull RD, Ritter JJ, Swartzendruder LJ. *J. Appl. Phys.* 1991; **69**: 54 144.
5. Borelli NF, Morse DL, Schreurs JWH. *J. Appl. Phys.* 1983; **54**: 3344.
6. Fröba M, Köhn R, Bouffaud G, Richard O, van Tendeloo G. *Chem. Mater.* 1999; **11**: 2858.
7. Raymond L, Revol J-F, Ryan DH, Marchessault RH. *J. Appl. Polym. Sci.* 1996; **59**: 1073.
8. Ziolo RF, Giannelis EP, Weinstein BA, O'Horo MP, Ganguly BN, Mehrotra V, Russell MW, Huffman DR. *Science* 1992; **257**: 219.
9. Okada H, Sakata K, Kunitake T. *Chem. Mater.* 1990; **2**: 89.
10. Sobon CA, Bowen HK, Broad A, Calvert PD. *J. Mater. Sci. Lett.* 1987; **6**: 901.
11. Chen L, Yang WJ, Yang CZ. *J. Mater. Sci.* 1997; **32**: 3571.
12. Kryszewski M, Jeszka JK. *Synth. Met.* 1998; **94**: 99.

13. Sohn BH, Cohen RE. *Chem. Mater.* 1997; **9**: 264.
14. Mayer CR, Cabuil V, Lalot T, Thouvenot R. *Angew. Chem. Int. Ed. Engl.* 1999; **38**: 3672.
15. Kumar RV, Koltypin Yu, Cohen YS, Cohen Y, Aurbach D, Palchik O, Felner I, Gedanken A. *J. Mater. Chem.* 2000; **10**: 1125.
16. Nustad KS, Funderud TE, Berge A, Ugelstad J. In *Scientific Methods for the Study of Polymer Colloids and their Applications*, Candau F, Ottewill RH (eds). Kluwer Academic: Dordrecht, 1990; 517.
17. Vladimir SZ, Filimonov DS, Presnyakov IA, Gambino RJ, Chu B. *J. Colloid Interface Sci.* 1999; **49**: 212.
18. Dresco PA, Vladimir SZ, Gambino RJ, Chu B. *Langmuir* 1999; **15**: 1945.
19. El-Shall MS. *Appl. Surf. Sci.* 1996; **106**: 347 and references cited therein.
20. De Caro D, Ely TO, Mari A, Chaudret B. *Chem. Mater.* 1996; **8**: 1987.
21. Majima Ishii TT, Matsumoto Y, Takami M. *J. Am. Chem. Soc.* 1989; **111**: 2417.
22. Veintemillas-Verdaguer S, Bomati O, Morales MP, Di Nunzio PE, Martelli S. *Mater. Lett.* 2003; **57**: 1184.
23. Huisken F, Kohn B, Alexandrescu R, Morjan I. *J. Chem. Phys.* 2000; **113**: 6579.
24. Hofmeister H, Huisken F, Kohn B, Alexandrescu R, Cojocaru S, Cruntenanu A, Morjan I, Diamandescu L. *Appl. Phys. A* 2001; **72**: 7.
25. Bomati Miguel O, Morales MP, Serna CJ, Veintemillas-Verdaguer S. *IEEE Trans. Magn.* 2002; **38**: 2616.
26. Veintemillas-Verdaguer S, Morales MP, Serna CJ. *Appl. Organometal. Chem.* 2001; **15**: 365.
27. Alexandrescu R, Morjan I, Crunteanu A, Cojocaru S, Petcu S, Teodorescu V, Huisken F, Kohn B, Ehbrecht M. *Mater. Chem. Phys.* 1998; **55**: 115.
28. Martelli S, Mancici A, Giorgi R, Alexandrescu R, Cojocaru S, Crunteanu A, Voicu I, Balu M, Morjan I. *Appl. Surf. Sci.* 2000; **154–155**: 353.
29. Pola J, Urbanová M, Volnina EA, Bakardjieva S, Šubrt J, Bastl Z. *J. Mater. Chem.* 2003; **13**: 394.
30. Frurip DJ, Staszak PR, Blander M. *J. Non-cryst. Solids* 1984; **68**: 1.
31. Martelli S, Bomati-Miguel O, de Dominicis L, Giorgi R, Rinaldi F, Veintemillas-Verdaguer S. *Appl. Surf. Sci.* 2002; **186**: 562.
32. Fajgar R, Bastl Z, Šubrt J, Vacek K, Pola J. *Phys. Chem. Chem. Phys.* 2003; **5**: 3789.
33. Sawada Y, Kageyama Y, Iwata M, Tasaki A. *Jpn. J. Appl. Phys.* 1992; **31**: 3858.
34. Urbanová M, Bastl Z, Šubrt J, Pola J. *J. Mater. Chem.* 2001; **11**: 1557.
35. Pola J, Ouchi A, Bastl Z, Šubrt J, Sakuragi M, Galiková A, Galík A. *Adv. Mater. Chem. Vap. Deposit.* 2001; **7**: 19.
36. Pola J, Urbanová M, Bastl Z, Šubrt J, Beckers H. *J. Mater. Chem.* 1999; **9**: 2429.
37. Pola J, Bastl Z, Urbanová M, Šubrt J, Beckers H. *Appl. Organometal. Chem.* 2000; **14**: 453.
38. Pola J, Galíkova A, Galík A, Blechta V, Bastl Z, Šubrt J, Ouchi A. *Chem. Mater.* 2002; **14**: 144.
39. Pola J, Kupčík J, Blechta V, Galíková A, Galík A, Šubrt J, Kurjata J, Chojnowski J. *Chem. Mater.* 2002; **14**: 1242.
40. Pola J, Ouchi A, Vacek K, Galikova A, Blechta V, Boháček J. *Solid State Sci.* 2003; **5**: 1079.
41. Pola J, Tomovska R, Bakardjieva S, Galíková A, Vacek K, Galík A. *J. Non-cryst. Solids* 2003; **328**: 227.
42. Shaub WM, Bauer SH. *Int. J. Chem. Kinet.* 1975; **7**: 509.
43. Russell DK. *Chem. Soc. Rev.* 1990; **19**: 407.
44. Pola J. *Spectrochim. Acta Sect. A* 1990; **46**: 607.
45. Pola J, Alexandrescu R, Morjan I, Sorescu D. *J. Anal. Appl. Pyrol.* 1990; **18**: 71.
46. Raabe G, Michl J. *Chem. Rev.* 1985; **85**: 419.
47. Miller RGJ, Willis HA (eds). *Infrared Structural Correlation Tables and Data Cards*. Heyden: London, 1969.
48. Nametkin NS, Oppengein VD, Zavyalov VI, Pushevaya SI, Vdovin VM. *Izv. Akad. Nauk SSSR Ser. Khim.* 1965; 1547; *Chem. Abstr.* 1966; **64**: 37 089d.
49. Morales MP, Veintemillas-Verdauguer S, Montero MI, Serna CJ, Roig A, Casas L, Martinez B, Sanddiumenge F. *Chem. Mater.* 1999; **11**: 3058.
50. Oblonsky LJ, Devine TM. *Corros. Sci.* 1995; **37**: 17.
51. Baraton MI, Busca G, Prieto MC, Ricchiardi G, Escribano VS. *J. Solid State Chem.* 1994; **112**: 9.
52. Chen MS, Shen ZX, Liu XY, Wang J. *J. Mater. Res.* 2000; **15**: 483.
53. Andersson SLT, Howe RF. *J. Phys. Chem.* 1989; **93**: 4913.
54. Seyama H, Soma M. *J. Electron Spectrosc. Relat. Phenom.* 1987; **42**: 97.
55. Hawn DD, DeKoven BM. *Surf. Interface Anal.* 1987; **10**: 63.
56. Morra M, Occhiello E, Marola R, Garbassi F, Humprey P, Johnson D. *J. Colloid Interface Sci.* 1990; **137**: 11.
57. Shull RD, Bennett LH. *Nanostruct. Mater.* 1992; **1**: 83.
58. Tianshu Z, Hongmei L, Huamxing Z, Ruifang Z, Yusheng S. *Sensor. Actuat. B* 1996; **32**: 181.
59. Malyshev VV, Eryshkin AV, Koltypin EA, Varfolomeev AE, Vasiliev AA. *Sensor. Actuat. B* 1994; **18–19**: 434.
60. Han JS, Bredow T, Davey DE, Yu AB, Mulcahy DE. *Sensor. Actuat. B* 2001; **75**: 18.

